Atmospheric Transport and Bulk Deposition of Organochlorine Compounds at Leigongshan Nature Reserve in Southwest China

Jiayi Zhou[1,2], Libin Liu[3], Xin Xu[1], Yongfu Yu[4], Yang Li[4], Haiyan Zhang[5], Yue Xu[1*]

[1]State Key Laboratory of Environmental Geochemistry, Institute of Geochemistry, Chinese Academy of Sciences, Guiyang, 550002, China

[2]State Key Laboratory of Organic Geochemistry, Guangzhou Institute of Geochemistry, Chinese Academy of Sciences, Guangzhou, 510640, China

[3]College of Chemistry and Life Sciences, Zhejiang Normal University, Jinhua 321004, China

[4]Leigong Mountain National Nature Reserve Administration, Leishan 557100, China

[5]The Johns Hopkins University-Nanjing University Center for Chinese and American Studies, Nanjing University, Nanjing, 210093, China

Abstract

Atmospheric and bulk deposition samples collected at Leigongshan Nature Reserve (LNR) were analyzed to explore the status, transport, and deposition of atmospheric pollution—specifically, organochlorine compounds—in the foggy mountains of southwest China. Prohibition and restriction of persistent organic pollutants in the surrounding areas has led to a decline in organochlorine pesticides and polychlorinated biphenyls (PCBs), but not hexachlorobenzene (HCB), in the air. Wet deposition is a factor that strongly influences atmospheric input at LNR. Despite their relatively low atmospheric concentration levels, heavy precipitation could increase the deposition of hexachlorocyclohexanes (HCHs) and HCB in the summer. Air HCHs exhibited a "bimodal" pattern, with higher concentrations in spring and autumn and lower concentrations in summer. The low levels in summer are achieved at the expense of high surface input into the ground along their transport routes from South and Southeast Asia to southwest China. The HCB at LNR mainly originates from mainland China. The deposition fluxes are influenced by the enhanced washout of atmospheric particles in the rainy season and elevated particle-associated content in the winter. The potential sources of *o,p'*-DDT, *p,p'*-DDT, and PCBs are distributed widely over western low-latitudinal areas and eastern China. Atmospheric transport and deposition in spring and summer contributed to a significant proportion of the annual total fluxes when the air mass arrives from Southeast Asia, increasing rainfall at LNR. The foggy local weather might also enhance this deposition, eventually

* Corresponding author. Tel: 86-0851-8439-6941
E-*mail address*: xu-yue@mail.gyig.ac.cn

leading to the accumulation of pollutants at LNR.

Key words: Air transport; Bulk deposition; Foggy mountain; OCPs; PCBs

1. INTRODUCTION

Persistent organic pollutants (POPs) are a group of toxic, persistent, and bioaccumulative chemicals prohibited or restricted by a series of multilateral environmental agreements, such as the Stockholm Convention, the Basel Convention, and the Rotterdam Convention. Atmospheric transport and deposition are considered major pathways for the redistribution of these pollutants to pristine environments. To evaluate the air quality degeneration associated with POPs, air monitoring networks, such as the NJADN in New Jersey (Van Ry *et al.*, 2002; Gioia *et al.*, 2005), IDAN for the Great Lakes (Hoff *et al.*, 1996; Melymuk *et al.*, 2011), and the AMAP for the Arctic (Hung *et al.*, 2016), have been established for extensive monitoring. Local-scale observations have also been conducted in Germany (Bruckmann *et al.*, 2013), Sweden (Bergknut *et al.*, 2011), and other European countries (Carrera *et al.*, 2002; Arellano *et al.*, 2015; Jakobi *et al.*, 2015). Relevant research has also been conducted in China (Wong *et al.*, 2004; Yang *et al.*, 2012; Liu *et al.*, 2013; Guo *et al.*, 2017), but most study data have been obtained from urban or suburban areas relatively close to the pollution sources. These observations provide extensive historical and current information on variations in air quality, which is useful to assess the effectiveness of national and international chemical control initiatives (Hung *et al.*, 2016).

To effectively implement the Stockholm Convention, the Chinese government is taking measures to reduce and eliminate pesticide POPs, polychlorinated biphenyls (PCBs), and dioxins (SEPAC, 2007). Primary emissions of pesticides and PCBs generally shows a decreasing trend in China (Wang *et al.*, 2005; Cui *et al.*, 2015). However, current application or emission still dominates the air in low latitudinal areas such as Vietnam, India or the Bay of Bengal. Distinct seasonal changes in prevailing wind directions and precipitation patterns caused by the Indian monsoons may result in atmospheric transport from those sources to pristine areas in western China such as the Tibetan Plateau (Sheng *et al.*, 2013). Moreover, the emission of historical residues of POPs in eastern China could also influence relatively clean regions in the west. A numerical study identified the influences of pollution sources in eastern China and India on sink accumulation in southwest China (Xu *et al.*, 2013).Therefore, monitoring at the receptor sites in western China is essential to evaluate the pollution status and the transport and transfer processes.

In this paper, concurrent measurements of organochlorine pesticides (OCPs) and PCBs in both air and bulk deposition were performed at a mountaintop in Leigongshan Nature Reserve (LNR) of Guizhou Province, which is an important habitat for rare plant and animal species. Compared with the surrounding provinces, the historical usage of OCPs and PCBs are the lowest in Guizhou (Wang *et al.*, 2005). From a climatological perspective, this nature reserve, located within 100° and 110° E, delineates the South Asian and East Asian monsoon regions (Wang *et al.*, 2003); it thus has the potential to receive airborne pollutants transported from the regions lying

to its east and west. A numerical simulation of the environmental fate of α-HCH, performed after HCH restrictions were promulgated in Asia, suggested a potential sink in the surrounding areas (Xu *et al.*, 2013). Atmospheric observations at LNR may reveal the background air quality status in southwest China and the possible atmospheric transport routes. Bulk deposition together with air monitoring can be used to assess the atmospheric loadings and the link between transport and deposition.

2. METHODS

2.1. Sample collection and site description

Starting from January 6, 2016, atmospheric and deposition samples were collected for 1 year at the top of Leigongshan Mountain (26.389°N, 108.205°E; 2178 m above sea level), which is within LNR (Fig. S1). Located in Leishan County, Guizhou Province, this nature reserve covers an area of 47,300 ha, with 88% forest coverage. It is a temperate area with mild temperature, abundant rainfall, and vertical climate variation. The annual average temperature at the top of the mountain is approximately 9.4°C, and the annual precipitation is 1300 mm. The monthly average temperature and precipitation are plotted in Fig. S2. The mountain is foggy all year-round, with more than 300 foggy days each year. Because the mountaintop is characterized by dense fog and light drizzle, long-term dry deposition samples are difficult to obtain; thus, bulk atmospheric deposition samples were collected in this study.

Using a modified Anderson-type high-volume air sampler operated at a rate of 430 m^3 day^{-1}, 24-h air samples were collected once every 6 days. Atmospheric particulate and

gaseous samples were collected using quartz microfiber filters (QFFs) (Grade GF/A, 20.3 cm × 25.4 cm) and polyurethane foam (PUF) plugs (8.0 cm (length) × 6.25 cm (diameter)), respectively. Atmospheric bulk deposition samples were collected using stainless-steel funnels mounted 0.5 m above the ground. The continuous samples obtained within each month were combined, and the total monthly rainfall was measured using a calibrated jar. Deposition samples were filtered using glass microfiber filters (GMFs) (Grade GF/F, diameter = 4.7 cm) and passed through a chromatographic column containing a mixture of XAD-2 and XAD-4 (1:1) resin. Before sampling, the QFFs and GMFs were baked at 400°C for 4 h. The weights of the filters were measured before and after sampling. The PUFs and resin were precleaned twice in a Soxhlet apparatus by using acetone and dichloromethane (DCM), and these materials were kept frozen until use. The stainless-steel funnels for deposition sampling were cleaned using ethanol and DCM. The deposition samples were analyzed after storage, transportation, and filtration. The pollutants in the dissolved and particulate phases do not necessarily reflect the original phase partitioning because submicron particles might have passed through the 0.7-μm filter pores into the dissolved phase. Deposition was recorded as the sum of the target compound in the GMF and resin samples. Filters (QFFs and GMFs), PUFs, and resin columns were wrapped with clean aluminum foil, sealed in Teflon bags, and stored at −18°C until analysis.

2.2. Analytical procedures

Before laboratory analysis, QFFs and PUFs were spiked with internal standards, including 2,4,5,6-tetrachloro-m-xylene (TCmX), PCB-30, ^{13}C-PCB28, ^{13}C-PCB52, ^{13}C-PCB101, ^{13}C-PCB118, ^{13}C-PCB153, ^{13}C-PCB138, ^{13}C-PCB180, and PCB-209 as recovery surrogates, after which they were separately Soxhlet-extracted using DCM for 48 h. Deposition samples were also spiked with the same standards, filtered by GMFs and absorbed by XAD resin, and then Soxhlet-extracted using DCM for 48 h. The extracts were concentrated to a volume of 1 mL by using a rotary evaporator and solvent-exchanged into hexane. Extract purification was performed using an alumina/silica column containing anhydrous sodium sulfate, 50% sulfuric acid silica, neutral silica gel, and neutral alumina. The purified extracts were evaporated to approximately 100 μL under low nitrogen flow, following which 20 μL of dodecane was added. Samples were concentrated to the final volume of 20 μL. Then, ^{13}C-PCB141 was added to each sample as an internal standard for analyzing OCPs and PCBs.

In total, 47 chromatographic peaks corresponding to 32 PCB congeners (PCB-8, 28, 37, 44, 49, 52, 60, 66, 70, 74, 77, 82, 87, 99, 101, 105, 114, 118, 126, 128, 138, 153, 156, 158, 166, 169, 170, 179, 180, 183, 187, and 189) and 11 OCP compounds (HCB, α-HCH, β-HCH, γ-HCH, δ-HCH, and *o,p'*- and *p,p'*-DDE, -DDD and -DDT) were analyzed. The target compounds were detected and measured using an Agilent 7890/7000 GC-MS/MS in multiple reaction monitoring (MRM) mode with a capillary column (Varian, CP-Sil 8 CB, 50 m long, 0.25 mm ID, 0.25 μm thick). Sample (1 μL) was injected in splitless mode. The initial GC oven temperature was set at 80 °C for

0.5 min, raised to 160 °C at a rate of 20 °C min^{-1}, to 240 °C at a rate of 4 °C min^{-1}, to 295 °C at 10 °C min^{-1}, and finally held for 10 min. High purity helium was used as the carrier gas, with a flow rate of 1.0 mL min^{-1}. The instrumental settings of the GC-MS/MS were the same as those described by Huang *et al.* (2014) and Zheng *et al.* (2014).

2.3. QA/QC

The sampling and experimental procedures were controlled through tests of breakthrough, recovery, lab blanks, and field blanks. A breakthrough test was performed by placing a smaller PUF plug below the main PUF in the sampler. The smaller PUF trapped only 0%–3% of the compounds targeted in this study. Lab blanks were precleaned QFFs, GMFs, PUFs, and XAD resin. Filed blanks for collecting air samples were precleaned QFFs and PUFs exposed to ambient air for approximately 5 min, whereas those for the deposition samples were precleaned GMFs and XAD resins exposed to purified water at the sampling site. The lab and field blanks were stored and analyzed along with each batch of samples.

To determine the analytical recovery efficiencies, all collected samples were spiked with surrogates. The average recoveries of TCmX, PCB-30, ^{13}C-PCB28, ^{13}C-PCB52, ^{13}C-PCB101, ^{13}C-PCB118, ^{13}C-PCB153, ^{13}C-PCB138, ^{13}C-PCB180, and PCB-209 were 60% ± 9.6%, 70% ± 8.8%, 63% ± 4.1%, 72% ± 5.9%, 75% ± 4.7%, 74% ± 4.4%, 79% ± 8.3%, 82% ± 9.6%, 87% ± 13%, and 96% ± 14 %, respectively. Because the recoveries were relatively stable, the data were not recovery corrected. The

instrumental stability of GC-MS/MS was checked daily by using two series of OCP and PCB standards, and a relative standard deviation within ±15% was ensured. The instrumental detection limits (IDLs) were integrated where the signal-to-noise ratio was 3 in the chromatograms of samples. The method detection limits (MDLs) were derived from the mean concentrations of the target compounds of the field blanks, in units of mass plus three standard deviations (3σ). Target OCPs were not detected in field blanks of air particle samples. Target compounds in the field blanks ranged from less than the IDL to 0.17 ng for the other different matrixes employed in this study. For compounds less than the IDL in the field blanks, the MDL was defined as the IDL. The MDLs of the target PCBs and OCPs ranged from 0.002 to 1.1 pg m^{-3} for the air samples and from 0.05 to 2.5 pg L^{-1} for the water samples (Table S1). The quantities of compounds in the samples were blank-corrected.

2.4. Back-trajectory and potential source contribution function analysis

Air mass movement was estimated through trajectory analysis. For the sampling days, 5-day air parcel back-trajectories were calculated at 6-h intervals using Hybrid-Single Particle Integrated Trajectories (HYSPLIT 4.8) developed by the National Oceanic and Atmospheric Administration (NOAA) Air Resource Laboratory (http://www.arl.noaa.gov/HYSPLIT.php). Each trajectory was estimated at 500 m above ground level. Fig. S3 shows the monthly precipitation data from the Global Precipitation Climatology Centre provided by NOAA as well as the prevailing air mass backward trajectories clustered using HYSPLIT 4.8.

198 Potential source contribution function (PSCF) analysis (Hafner and Hites, 2003;
199 Hoh and Hites, 2004) was employed to illustrate the spatial distribution of the
200 potential sources. Back-trajectory lines are a series of points representing the position
201 of the modelled air mass at each hour. All the hourly points in the trajectories
202 generated by HYSPLIT 4.8 were sorted into 1° latitude × 1° longitude cells.
203 Accordingly, the PSCF of each grid is defined as follows:

204 $$PSCF = N_{high}/N_{all}$$

205 where N_{high} is the number of endpoints corresponding to the measured pollutant
206 concentrations higher than a given criterion threshold. In this study, all trajectories
207 corresponding to the chemical concentrations > average + 0.125 × standard deviations
208 were selected. N_{all} is the total number of endpoints falling in the grid cell. To avoid
209 numerical uncertainties, grid cells with $N_{all} < 10$ were excluded. The calculated PSCF
210 represents the probability of a given cell being a potential source region for a specific
211 observatory, rather than the strength of sources for a large region.

212

213 ***2.5. Deposition estimation***

214 Deposition fluxes were calculated assuming equilibrium status for the compounds
215 in the air and the rain. The predicted deposition fluxes are the sum of the dry particle
216 deposition (F_{dry}), the washout of particle phase (F_{part}), and the dissolved phase F_{diss}.

217 $$F_{dry} = C_{part} \times V_d \quad (1)$$

218 $$F_{part} = C_{part} \times rain \quad (2)$$

219 $$F_{diss} = C_{rain} \times rain = C_{gas} \times rain \times R \times T/H \quad (3)$$

where C_{part}, C_{gas}, and C_{rain} are the concentrations of the target compounds in the atmospheric particle phase, gaseous phase, and rainfall, respectively. V_d is the reported dry deposition rates (0.2 cm s^{-1}) (Hillery *et al.*, 1998; Miller *et al.*, 2001), *rain* is the precipitation intensity (m $month^{-1}$), R is the gas constant (8.314 Pa m^3 mol^{-1} K^{-1}), T is the temperature, and H is the temperature-dependent Henry's law constant (Mackay *et al.*, 2006).

3. RESULTS AND DISCUSSION

3.1. Pollution levels

Atmospheric OCPs and PCBs were mainly distributed in the gas phase of the air. The detection rate of the targeted 11 OCPs and 11 PCBs, including HCB, HCHs, DDTs, and PCB-8, -28, -37, -44, -52, -60, -66, -70, -74, -99, and -101, were >80% in the gas phase samples. Detection rates in the particle phase were generally <50%; hence, the air concentration results were calculated based on the total concentration. The average air concentration levels of OCPs and PCBs are summarized in Table S2. For compounds with concentration below the MDL, the mean concentration levels were calculated by assuming "not detected" data as equal to 1/3 MDL. Atmospheric OCP and PCB contamination at LNR is comparable with that recently reported for other regional background sites in China and worldwide (Table S2). The annual average concentrations of HCHs at LNR compare favorably with those at other background sites in China (Gong *et al.*, 2017; Zhan *et al.*, 2017), the Arctic (Bossi *et*

242 *al.*, 2016), and Sweden (Bidleman *et al.*, 2017), whereas DDT levels were lower than
243 those at other sites in China (Sheng *et al.*, 2013; Gong *et al.*, 2017; Zhan *et al.*, 2017)
244 and comparable with those at polar regions (Bossi *et al.*, 2016; Bidleman *et al.*, 2017)
245 and European high Alpine stations (Kirchner *et al.*, 2016). The mean HCB
246 concentration at LNR was lower than that reported in other studies, except for the
247 Tibetan Plateau (Sheng *et al.*, 2013; Gong *et al.*, 2017). Total PCB concentrations
248 (Σ_{32}PCB) ranged from 4.2 to 35 pg m^{-3}, with an average of 15 ± 7.2 pg m^{-3}. The
249 average contribution of di-, tri-, tetra-, penta-, hexa-, and hepta-CBs were 17%, 35%,
250 37%, 7.9%, 1.9%, and 0.7%, respectively. The concentrations of seven indicator
251 PCBs—namely PCB-28, -52, -101, -118, -138, -153, and -180—were compared with
252 those reported in the literature. The average concentration levels were relatively high
253 but lower than those found in central China (Zhan *et al.*, 2017). The atmospheric
254 concentrations of OCPs and PCBs at a background site in Guizhou Province were
255 evaluated in a passive air sampling (PAS) campaign conducted in 2004 (Jaward *et al.*,
256 2005); POPs sequestered through PAS were converted to air concentrations and are
257 listed in Table S2. Compared with data in 2004, air concentrations of DDTs and
258 high-molecular-weight PCBs reduced to low levels, whereas those of more volatile
259 compounds, such as HCB and low-molecular-weight PCBs, either showed a slight
260 declined or remained at the same levels.

261 The deposition concentrations at LNR were in the range reported at other remote
262 sites. Volume weighted mean (ng L^{-1}) concentrations in the deposition samples are
263 listed in Table S3. Of the 43 target compounds, the following 7 were commonly

detected in the deposition samples: HCB, α-HCH, γ-HCH, *p,p'*-DDT, *p,p'*-DDE, *o,p'*-DDT, and PCB-28. HCB, α-HCH, γ-HCH, and PCB-28 were found at relatively high concentrations. The average HCB concentration was within the range of 0.003 – 0.072 ng L^{-1}, which were observed in the United States national parks (Hageman *et al.*, 2006). HCHs concentrations were lower than the range of 1.8 – 5.0 ng L^{-1} obtained in French (Teil *et al.*, 2004) and Atlantic Canada background sites (Brun *et al.*, 2008). DDTs, including *p,p'*-DDT, *p,p'*-DDE, and *o,p'*-DDT, were found at a low level and also lower than those in Atlantic Canada (Brun *et al.*, 2008).

3.2. Effect of meteorological and atmospheric parameters

Meteorological and atmospheric factors, such as temperature, precipitation, wind direction, and particles, influence the air concentration (Wania *et al.*, 1998; Tian *et al.*, 2009) and deposition (Fernandez *et al.*, 2003) of POPs. Linear regressions of the logarithm of the concentrations of OCP or PCB gas in air versus reciprocal temperature (i.e., $\ln(C_{air}) = m/T + b$) are widely used to distinguish temperature-dependent volatilization from various surfaces. A strong temperature dependence of *p,p'*-DDE was observed, with a high R^2 of 0.66 (Fig. S4), suggesting that this compound is mainly influenced by volatilization. The correlation between ln C and 1/T of the other compounds were either nonsignificant ($p > 0.05$) or weak ($p < 0.05$ and $R^2 < 0.2$), indicating that at LNR, revolatilization from nearby surfaces may not be the major source of most OCPs and PCBs in the atmosphere. The correlation between air concentrations and precipitation was nonsignificant.

286 The effect of temperature and precipitation on deposition was investigated through
287 linear regression analysis. A significant negative relationship was observed between
288 $\ln(C_{dep})$ of HCB and temperature (Fig. S5). This relationship is likely related to the
289 tendency of atmospheric HCB to partition into particles during cold seasons given that
290 HCB concentrations in the atmospheric particles increased in cold seasons (Fig. S6).
291 The correlation between the concentrations of target compounds in the deposition
292 samples and the total suspended particles was nevertheless nonsignificant. For α- and
293 γ-HCH with relatively high water solubilities, significant high correlation coefficients
294 of 0.97 and 0.92, were observed between precipitation and monthly deposition fluxes,
295 respectively.
296
297 ***3.3. Transport and deposition trend of OCPs and PCBs***
298 The movement of airborne pollutants to remote areas entails three essential
299 parameters, namely source emission, transport route, and favorable deposition
300 condition at the receptor site. The following sections discuss the influence of these
301 parameters on pollutant transport and deposition at LNR.
302
303 3.3.1 HCHs
304 The seasonality of HCHs exhibited a "bimodal" pattern, with higher concentrations
305 in spring and autumn and lower concentrations in summer (Fig. 1). Regarding other
306 sites in the same latitudinal zone (Fig. S1; location details of the Tibetan and central
307 China sites are shown in Table S1), this pattern was observed at the Tibetan Plateau

but not at the central China site. Sheng *et al.* (2013) correlated this bimodal pattern to agricultural input of HCHs from India and rain scavenging in the rainy season. Zhan *et al.* (2017) attributed the high HCH levels in central China during winter to polluted air parcels originating from northern China. PSCF maps of α- and γ-HCH reveal that northern China, Southeast Asia, and the Bay of Bengal are potential sources of HCHs in this study (Fig. S7). Most air parcels arriving at LNR passed through these potential sources from March to September (Fig. S3). The atmospheric concentrations of HCHs were high in March, April, and September and low from May to August, when many trajectories passed through precipitation centers over the Bay of Bengal and the South China Sea (Fig. S3, May to August).

For POPs with significant water solubility, such as α- and γ-HCH, rainfall scavenging in the rainy season is a particularly effective method to remove these compounds from the air. The annual total α- and γ-HCH deposition fluxes were 82 and 114 ng m^{-2}, with atmospheric deposition fluxes from May to August contributing 60% and 68%, respectively; the relatively low air concentrations during these periods are likely achieved at the expense of high deposition from the air to the ground surface along the transport routes. The water solubility of γ-HCH (7.3 mg L^{-1}) is higher than that of α-HCH (1.5 mg L^{-1}) (Mackay *et al.*, 2006); hence, wet deposition is more effective for γ-HCH and even significantly influences the α-/γ-HCH ratio, a source indicator. Between May and July, the average α-/γ-HCH ratio was 2.7 in the atmospheric samples, whereas it was only 0.62 in the deposition samples. For air samples, the average ratio increased from 2.2 in April to 3.1 in May, despite the

similarity of the air mass back-trajectories of these two months. These results imply that using isomer ratio indicators to distinguish between sources of relatively highly water-soluble compounds is difficult if the air mass passes through precipitation centers, such as the Bay of Bengal and the South China Sea. For example, the atmospheric α-/γ-HCH ratios indicate technical HCH usage in the mainland of China, Vietnam, and the Kolkata region of India (Chakraborty *et al.*, 2010; Wang *et al.*, 2016) or Lindane use in the China Sea and the Bay of Bengal (Gioia *et al.*, 2012). Intensive precipitation over the sea areas may reduce the Lindane signals in the atmosphere when the air mass arrives at downwind receptors, such as at Tibetan and LNR sites.

3.3.2 HCB

HCB concentration exhibited clear seasonal variations, with elevated concentrations in winter months (Fig. 2), which was also reported in central China (Zhan *et al.*, 2017), the Tibetan Plateau (Sheng *et al.*, 2013), and other observation areas (Wang *et al.*, 2010). Decreasing the atmospheric concentration of HCB is difficult. Comparing the concentrations at the sites shown in Fig. S1, the annual average concentrations of HCB gradually decreased from east to west, with the highest in central China and the lowest in the Tibetan Plateau (Table S2). This spatial trend suggests that potential sources of HCB are likely located in central and eastern China. The PSCF map of HCB supports this assumption by indicating that the potential sources are widely distributed in southeast, central, and northern China (Fig. S8). This spatial pattern is similar to that of air HCB measured in 2004 (Jaward *et al.*,

2005), suggesting that HCB concentrations at LNR are still influenced by these source regions, especially in the cold season.

The annual HCB deposition flux of 52.1 ng m^{-2} was close to those reported at other background sites (Arellano *et al.*, 2015). Elevated HCB deposition fluxes occurred not only in winter but also in summer (Fig. 2). The high fluxes in winter are mainly associated with elevated particle-associated HCB content in the air (Fig. S9). To a less significant extent, elevated gaseous HCB and TSP in the air, may be related to high fluxes in winter. Unlike HCHs, HCB is a volatile compound with low water solubility, meaning that the HCB dissolution in rainwater during summertime is nonsignificant. The high concentrations in June and August likely reflect the enhanced washout of atmospheric particles during the rainy season.

3.3.3 DDTs

Seasonality was exhibited by *o,p'*-DDT and *p,p'*-DDT, with higher concentrations in spring and lower concentrations in winter (Fig. 3), which is quite different from the pattern observed for atmospheric DDTs at sites in the Tibetan Plateau and central China, which exhibited high levels in summer (Sheng *et al.*, 2013; Zhan *et al.*, 2017). The variation of *p,p'*-DDE at LNR was significantly correlated with temperature and therefore peaked in July (Fig. S10). By contrast, the highest mean concentrations of *o,p'*-DDT and *p,p'*-DDT were recorded in April. The potential source regions of *o,p'*-DDT are distributed in Southeast Asia, whereas those of *p,p'*-DDT include Southeast Asia and eastern China (Fig. S11). The ratio of *o,p'*-DDT to *p,p'*-DDT, an

indicator of DDT sources for technical DDT and dicofol, was 0.98 ± 0.58 at LNR; this is consistent with the technical DDT use reported in Vietnam (Zhan *et al.*, 2017) and eastern China (Liu *et al.*, 2009).

Atmospheric fluxes of *o,p'*-DDT and *p,p'*-DDT peaked in April, accounting for 30% of the annual total fluxes. The deposition of DDTs with high K_{oa} is mainly controlled by atmospheric particles (Yue *et al.*, 2011). The observed deposition fluxes also follow the seasonality of particle-associated DDT concentrations (Fig. S12). In April, the air mass mainly originated from Southeast Asia, before precipitation centers had formed over the oceans (Fig. S3, April); nevertheless, rainfall at LNR started to increase (Fig. S2), which was favorable for atmospheric deposition. By contrast, the low DDT content in the particles and the precipitation amount led to relatively low depositions in cold seasons (Fig. S12); this is despite the air mass occasionally passing through potential source regions in eastern China in cold seasons, bringing about *p,p'*-DDT pollution.

3.3.4 PCBs

PCB congeners exhibited similar temporal trends, with high concentrations observed from April to August. The potential sources are presented in the PSCF maps in Fig. S13. The sources of tri-CBs are likely located in lower latitudinal areas, while those of tetra- and penta-CBs are distributed in central China as well. The map for hex-CBs exclusively displays a few clusters of high-probability cells over central China. Although relevant data on the source regions are limited, the air concentration

396 levels of PCBs in Vietnam (Wang *et al.*, 2016) and India (Chakraborty *et al.*, 2013)
397 has been reported to be higher than those in other Asian countries. The high
398 atmospheric PCB concentrations over the South China Seas and the Bay of Bengal
399 (Gioia *et al.*, 2012) could also contribute to PCB transport. PCB-28 was the only PCB
400 congener detected in all deposition samples. The trends in monthly deposition fluxes
401 were similar to those of air concentration (Fig. S14): the deposition flux was high in
402 the rainy season, when air mass mainly arrived from the west.
403
404 3.3.5 Comparison of measured and predicted deposition fluxes
405 Fig. 4 compares the measured and predicted deposition fluxes at LNR. The
406 similarity between the measured and predicted seasonal trends suggests a strong link
407 between atmospheric input and deposition. The measured deposition fluxes were
408 generally higher than the predicted equilibrium fluxes, except for compounds whose
409 concentrations were close to the MDL, such as *o,p'*-DDT. Numerous studies have
410 suggested that fog, clouds, and snow at high altitudes can scavenge organic pollutants
411 from the atmosphere, often more efficiently than rain (Jakobi *et al.*, 2015). At LNR,
412 our sampling site is a low-latitudinal site characterized by foggy weather. We suspect
413 that the fog may induce higher deposition. In a previous numerical simulation, the
414 α-HCH sink in southwest China was found to be related to atmospheric transport and
415 strong deposition in the rainy season (Xu *et al.*, 2013). The measured deposition
416 fluxes at LNR being higher than predicted indicates that deposition input in the
417 surrounding areas might be even higher than previously estimated.

4. CONCLUSIONS

The atmospheric transport and deposition of OCPs and PCBs at LNR, a nature reserve in southwest China, were investigated. Governments in Asia have prohibited or restricted POPs, as stipulated in the Stockholm Convention; consequently, atmospheric concentrations of POPs, except HCB, have exhibited a declining trend. Nevertheless, the temporal shift of the wind field could transport pollutants from surrounding sources, such as mainland China and South and Southeast Asia to LNR. Wet deposition, including that in the dissolved and particulate phases, serves as an effective transfer route. The atmospheric transport and deposition of compounds with relatively high water solubility, such as HCHs, in the rainy season contributed to a significant proportion of the air input. During this season, air masses mainly originate from western source areas. The low pollution atmospheric levels at LNR are likely achieved at the expense of high surface input along the transport routes. For other compounds, the washouts of particles by precipitation also influenced their total deposition. HCB and DDT deposition followed the temporal variations of their particle-associated content, with the highest deposition fluxes occurring in winter and April, respectively. Except for DDTs, the measured deposition fluxes were higher than the predicted equilibrium fluxes for all compounds; this could be related to the foggy weather at LNR.

ACKNOWLEDGMENTS

The authors appreciate the financial support from the National Natural Science Foundation of China (NSFC) (41403106, 414300417, 41673133, 71403118, and 41101495) and National Key R&D Program of China (ATMSYC, 2017YFC0212000). Author contributions: conceptualization: Jiayi Zhou and Yue Xu; sample and data analysis: Jiayi Zhou, Libin Liu, and Xin Xu; sample collection: Yongfu Yu and Yang Li; writing, review, and editing: Haiyan Zhang and Yue Xu. This manuscript was edited by Wallace Academic Editing.

REFERENCES

Arellano, L., Fernandez, P., Fonts, R., Rose, N.L., Nickus, U., Thies, H., Stuchlik, E., Camarero, L., Catalan, J. and Grimalt, J.O. (2015). Increasing and decreasing trends of the atmospheric deposition of organochlorine compounds in European remote areas during the last decade. *Atmospheric Chemistry and Physics* 15: 6069-6085.

Bergknut, M., Laudon, H., Jansson, S., Larsson, A., Gocht, T. and Wiberg, K. (2011). Atmospheric deposition, retention, and stream export of dioxins and PCBs in a pristine boreal catchment. *Environ. Pollut.* 159: 1592-1598.

Bidleman, T.F., Laudon, H., Nygren, O., Svanberg, S. and Tysklind, M. (2017). Chlorinated pesticides and natural brominated anisoles in air at three northern Baltic stations. *Environ. Pollut.* 225: 381-389.

Bossi, R., Vorkamp, K. and Skov, H. (2016). Concentrations of organochlorine pesticides, polybrominated diphenyl ethers and perfluorinated compounds in the atmosphere of north Greenland. *Environ. Pollut.* 217: 4-10.

Bruckmann, P., Hiester, E., Klees, M. and Zetzsch, C. (2013). Trends of PCDD/F and PCB concentrations and depositions in ambient air in northwestern Germany. *Chemosphere* 93: 1471-1478.

Brun, G.L., MacDonald, R.M., Verge, J. and Aubé, J. (2008). Long-term atmospheric deposition of current-use and banned pesticides in Atlantic Canada; 1980–2000. *Chemosphere* 71: 314-327.

Carrera, G., Fernández, P., Grimalt, J.O., Ventura, M., Camarero, L., Catalan, J., Nickus, U., Thies, H. and Psenner, R. (2002). Atmospheric deposition of organochlorine compounds to remote high mountain lakes of Europe. *Environ. Sci. Technol.* 36: 2581-2588.

Chakraborty, P., Zhang, G., Eckhardt, S., Li, J., Breivik, K., Lam, P.K.S., Tanabe, S. and Jones, K.C. (2013). Atmospheric polychlorinated biphenyls in Indian cities: Levels, emission sources and toxicity equivalents. *Environ. Pollut.* 182: 283-290.

Chakraborty, P., Zhang, G., Li, J., Xu, Y., Liu, X., Tanabe, S. and Jones, K.C. (2010). Selected organochlorine pesticides in the atmosphere of major Indian cities: Levels, regional versus local variations, and sources. *Environ. Sci. Technol.* 44: 8038-8043.

Cui, S., Fu, Q., Ma, W.L., Song, W.W., Liu, L.Y. and Li, Y.F. (2015). A preliminary compilation and evaluation of a comprehensive emission inventory for polychlorinated biphenyls in China. *Sci. Total Environ.* 533: 247-255.

Fernandez, P., Carrera, G., Grimalt, J.O., Ventura, M., Camarero, L., Catalan, J., Nickus, U., Thies, H. and Psenner, R. (2003). Factors governing the atmospheric deposition of polycyclic aromatic hydrocarbons to remote areas. *Environ. Sci. Technol.* 37: 3261-3267.

Gioia, R., Li, J., Schuster, J., Zhang, Y.L., Zhang, G., Li, X.D., Spiro, B., Bhatia, R.S., Dachs, J. and Jones, K.C. (2012). Factors affecting the occurrence and transport of atmospheric organochlorines in the China Sea and the northern Indian and South east Atlantic oceans. *Environ. Sci. Technol.* 46: 10012-10021.

Gioia, R., Offenberg, J.H., Gigliotti, C.L., Totten, L.A., Du, S. and Eisenreich, S.J. (2005). Atmospheric concentrations and deposition of organochlorine pesticides in the US Mid-Atlantic region. *Atmos. Environ.* 39: 2309-2322.

Gong, P., Wang, X., Sheng, J., Wang, H., Yuan, X., He, Y., Qian, Y. and Yao, T. (2017). Seasonal variations and sources of atmospheric polycyclic aromatic hydrocarbons and organochlorine compounds in a high-altitude city: Evidence from four-year observations. *Environ. Pollut.*

Guo, L.-C., Bao, L.-J., Li, S.-M., Tao, S. and Zeng, E.Y. (2017). Evaluating the effectiveness of pollution control measures via the occurrence of DDTs and HCHs in wet deposition of an urban center, China. *Environ. Pollut.* 223: 170-177.

Hafner, W.D. and Hites, R.A. (2003). Potential sources of pesticides, PCBs, and PAHs to the atmosphere of the Great Lakes. *Environ. Sci. Technol.* 37: 3764-3773.

Hageman, K.J., Simonich, S.L., Campbell, D.H., Wilson, G.R. and Landers, D.H. (2006). Atmospheric deposition of current-use and historic-use pesticides in snow at national parks in the western United States. *Environ. Sci. Technol.* 40: 3174-3180

Hillery, B.R., Simcik, M.F., Basu, I., Hoff, R.M., Strachan, W.M.J., Burniston, D., Chan, C.H., Brice, K.A., Sweet, C.W. and Hites, R.A. (1998). Atmospheric deposition of toxic pollutants to the Great Lakes as measured by the integrated atmospheric deposition network. *Environ. Sci. Technol.* 32: 2216-2221.

Hoff, R.M., Strachan, W.M.J., Sweet, C.W., Chan, C.H., Shackleton, M., Bidleman, T.F., Brice, K.A., Burniston, D.A., Cussion, S., Gatz, D.F., Harlin, K. and Schroeder, W.H. (1996). Atmospheric deposition of toxic chemicals to the Great Lakes: A review of data through 1994. *Atmos. Environ.* 30: 3505-3527.

Hoh, E. and Hites, R.A. (2004). Sources of toxaphene and other organochlorine pesticides in North America as determined by air measurements and potential source contribution function analyses. *Environ. Sci. Technol.* 38: 4187-4194.

Huang, Y., Li, J., Xu, Y., Xu, W., Cheng, Z., Liu, J., Wang, Y., Tian, C., Luo, C. and Zhang, G. (2014). Polychlorinated biphenyls (PCBs) and hexachlorobenzene (HCB) in the equatorial Indian Ocean: Temporal trend, continental outflow and air–water exchange. *Mar. Pollut. Bull.* 80:

194-199.

Hung, H., Katsoyiannis, A.A., Brorström-Lundén, E., Olafsdottir, K., Aas, W., Breivik, K., Bohlin-Nizzetto, P., Sigurdsson, A., Hakola, H., Bossi, R., Skov, H., Sverko, E., Barresi, E., Fellin, P. and Wilson, S. (2016). Temporal trends of persistent organic pollutants (POPs) in Arctic air: 20 years of monitoring under the Arctic Monitoring and Assessment Programme (AMAP). *Environ. Pollut.* 217: 52-61.

Jakobi, G., Kirchner, M., Henkelmann, B., Körner, W., Offenthaler, I., Moche, W., Weiss, P., Schaub, M. and Schramm, K.-W. (2015). Atmospheric bulk deposition measurements of organochlorine pesticides at three alpine summits. *Atmos. Environ.* 101: 158-165.

Jaward, T.M., Zhang, G., Nam, J.J., Sweetman, A.J., Obbard, J.P., Kobara, Y. and Jones, K.C. (2005). Passive air sampling of polychlorinated biphenyls, organochlorine compounds, and polybrominated diphenyl ethers across Asia. *Environ. Sci. Technol.* 39: 8638-8645.

Kirchner, M., Jakobi, G., Körner, W., Levy, W., Moche, W., Niedermoser, B., Schaub, M., Ries, L., Weiss, P., Antritter, F., Fischer, N., Henkelmann, B. and Schramm, K.-W. (2016). Ambient air levels of organochlorine pesticides at three high alpine monitoring stations: Trends and dependencies on geographical origin. *Aerosol and Air Quality Research* 16: 738-751.

Liu, F., Xu, Y., Liu, J., Liu, D., Li, J., Zhang, G., Li, X., Zou, S. and Lai, S. (2013). Atmospheric deposition of polycyclic aromatic hydrocarbons (PAHs) to a coastal site of Hong Kong, South China. *Atmos. Environ.* 69: 265-272.

Liu, X., Zhang, G., Li, J., Yu, L.L., Xu, Y., Li, X.D., Kobara, Y. and Jones, K.C. (2009). Seasonal patterns and current sources of DDTs, chlordanes, hexachlorobenzene, and endosulfan in the atmosphere of 37 Chinese cities. *Environ. Sci. Technol.* 43: 1316-1321.

Mackay, D., Shiu, W.Y., Ma, K.C. and Lee, S.C. (2006). *Handbook of physical-chemical properties and environmental fate for organic chemicals*, 2nd ed. CRC Press, Boca Raton.

Melymuk, L., Robson, M., Diamond, M.L., Bradley, L.E. and Backus, S. (2011). Wet deposition loadings of organic contaminants to Lake Ontario: Assessing the influence of precipitation from urban and rural sites. *Atmos. Environ.* 45: 5042-5049.

Miller, S.M., Green, M.L., DePinto, J.V. and Hornbuckle, K.C. (2001). Results from the Lake Michigan mass balance study: Concentrations and fluxes of atmospheric polychlorinated biphenyls and trans-nonachlor. *Environ. Sci. Technol.* 35: 278-285.

SEPAC (2007). National implementation plan for the Stockholm Convention on persistent organic pollutants State Environmental Protection Administration of China.

Sheng, J.J., Wang, X.P., Gong, P., Joswiak, D.R., Tian, L.D., Yao, T.D. and Jones, K.C. (2013). Monsoon-driven transport of organochlorine pesticides and polychlorinated biphenyls to the Tibetan Plateau: Three year atmospheric monitoring study. *Environ. Sci. Technol.* 47: 3199-3208.

Teil, M.J., Blanchard, M. and Chevreuil, M. (2004). Atmospheric deposition of organochlorines (PCBs and pesticides) in northern France. *Chemosphere* 55: 501-514.

Tian, C., Ma, J., Liu, L., Jia, H., Xu, D. and Li, Y.-F. (2009). A modeling assessment of association between East Asian summer monsoon and fate/outflow of α-HCH in Northeast Asia. *Atmos. Environ.* 43: 3891-3901.

Van Ry, D.A., Gigliotti, C.L., Glenn, T.R., Nelson, E.D., Totten, L.A. and Eisenreich, S.J. (2002). Wet deposition of polychlorinated biphenyls in urban and background areas of the mid-Atlantic states. *Environ. Sci. Technol.* 36: 3201-3209.

Wang, B., Clemens, S.C. and Liu, P. (2003). Contrasting the Indian and East Asian monsoons: Implications on geologic timescales. *Mar. Geol.* 201: 5-21.

Wang, G., Lu, Y., Han, J., Luo, W., Shi, Y., Wang, T. and Sun, Y. (2010). Hexachlorobenzene sources, levels and human exposure in the environment of China. *Environ. Int.* 36: 122-130.

Wang, T., Lu, Y., Zhang, H. and Shi, Y. (2005). Contamination of persistent organic pollutants (POPs) and relevant management in China. *Environ. Int.* 31: 813-821.

Wang, W., Wang, Y., Zhang, R., Wang, S., Wei, C., Chaemfa, C., Li, J., Zhang, G. and Yu, K. (2016). Seasonal characteristics and current sources of OCPs and PCBs and enantiomeric signatures of chiral OCPs in the atmosphere of Vietnam. *Sci. Total Environ.* 542: 777-786.

Wania, F., Haugen, J.-E., Lei, Y.D. and Mackay, D. (1998). Temperature dependence of atmospheric concentrations of semivolatile organic compounds. *Environ. Sci. Technol.* 32: 1013-1021.

Wong, H.L., Giesy, J.P. and Lam, P.K.S. (2004). Atmospheric deposition and fluxes of organochlorine pesticides and coplanar polychlorinated biphenyls in aquatic environments of Hong Kong, China. *Environ. Sci. Technol.* 38: 6513-6521.

Xu, Y., Tian, C., Zhang, G., Ming, L., Wang, Y., Chen, Y., Tang, J., Li, J. and Luo, C. (2013). Influence of monsoon system on alpha-HCH fate in Asia: A model study from 1948 to 2008. *Journal of Geophysical Research-Atmospheres* 118: 6764-6770.

Yang, G., Ma, L., Xu, D., Liu, L., Jia, H., Chen, Y., Zhang, Y. and Chai, Z. (2012). Temporal trends of polychlorinated biphenyls in precipitation in Beijing, China. *Atmos. Environ.* 56: 222-227.

Yue, Q., Zhang, K., Zhang, B.-Z., Li, S.-M. and Zeng, E.Y. (2011). Occurrence, phase distribution and depositional intensity of dichlorodiphenyltrichloroethane (DDT) and its metabolites in air and precipitation of the Pearl River Delta, China. *Chemosphere* 84: 446-451.

Zhan, L., Lin, T., Wang, Z., Cheng, Z., Zhang, G., Lyu, X. and Cheng, H. (2017). Occurrence and air–soil exchange of organochlorine pesticides and polychlorinated biphenyls at a CAWNET background site in central China: Implications for influencing factors and fate. *Chemosphere* 186: 475-487.

Zheng, Q., Nizzetto, L., Mulder, M., Sáňka, O., Lammel, G., Li, J., Bing, H.J., Liu, X., Jiang, Y.S. and Zhang, G. (2014). Does an analysis of polychlorinated biphenyl (PCB) distribution in mountain soils across China reveal a latitudinal fractionation paradox? *Environ. Pollut.* 195: 115-122.

Figure Captions

Fig. 1. Seasonality of monthly mean air concentrations and deposition fluxes of α-HCH (A) and γ-HCH (B)

Fig. 2. Seasonality of monthly mean air concentrations and deposition fluxes of HCB

Fig. 3. Seasonality of monthly mean air concentrations and deposition fluxes of *o,p'*-DDT (A) and *p,p'*-DDT (B)

Fig. 4. Measured and predicted deposition fluxes at LNR

601

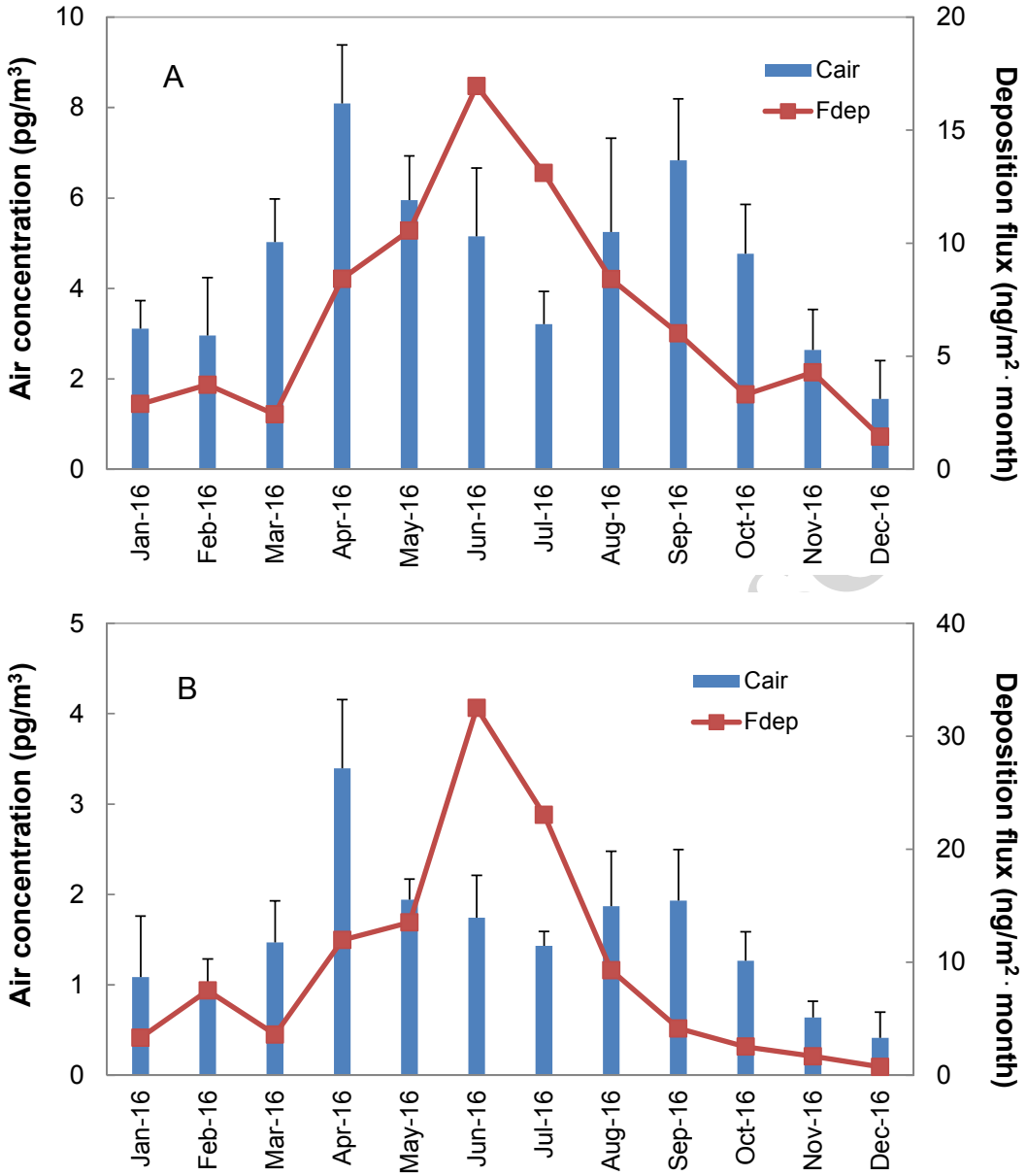

602

603 Fig. 1. Seasonality of monthly mean air concentrations and deposition fluxes of α-HCH (A) and
604 γ-HCH (B)

605

606

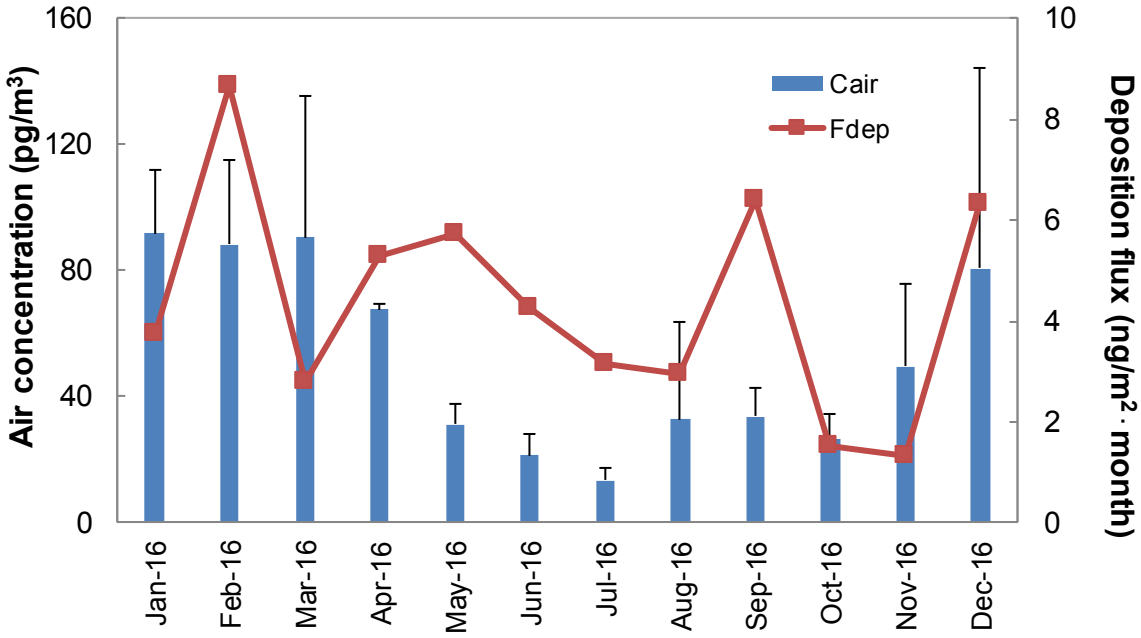

607
608 Fig. 2. Seasonality of monthly mean air concentrations and deposition fluxes of HCB
609
610

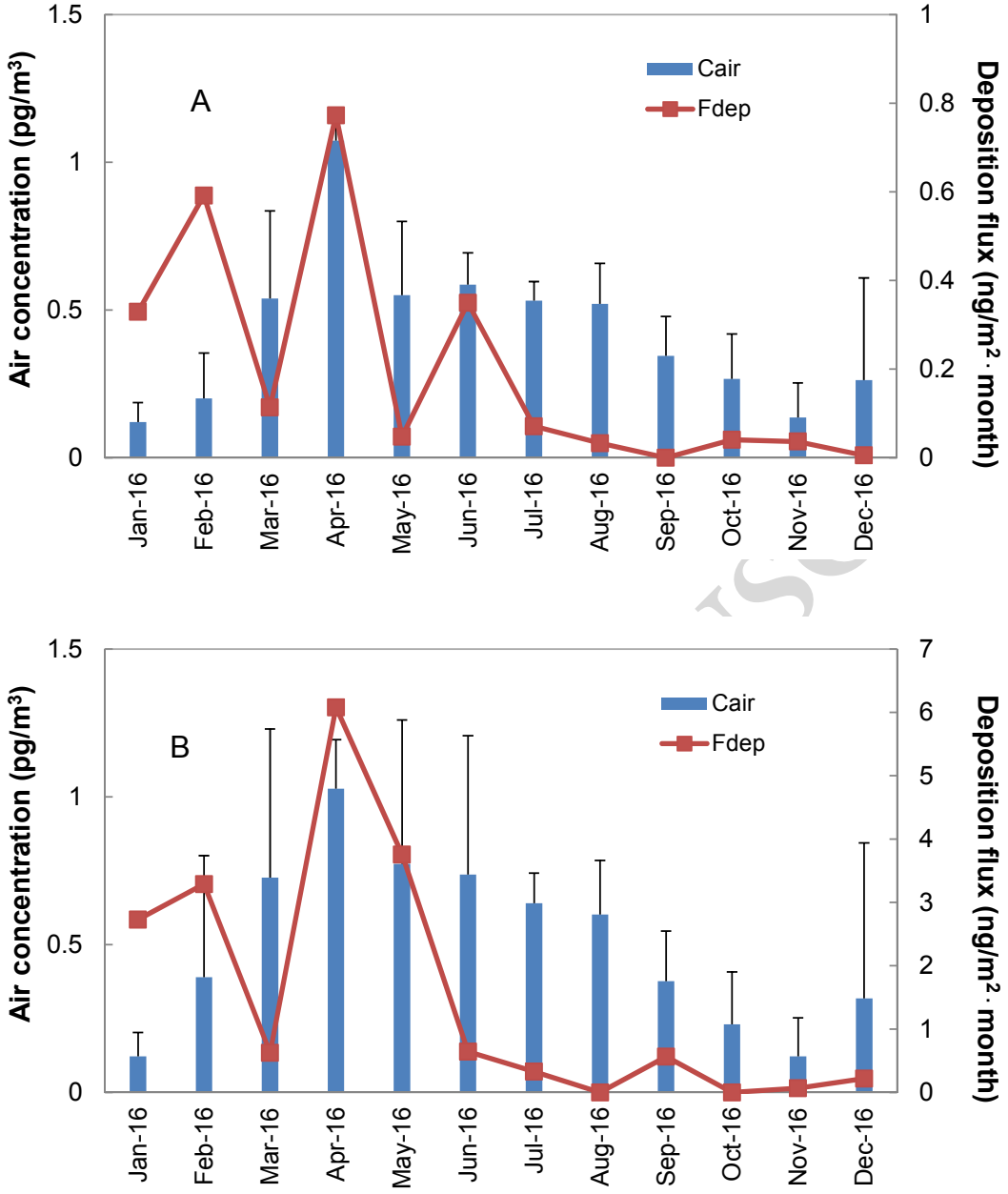

Fig. 3. Seasonality of monthly mean air concentrations and deposition fluxes of *o,p'*-DDT (A) and *p,p'*-DDT (B)

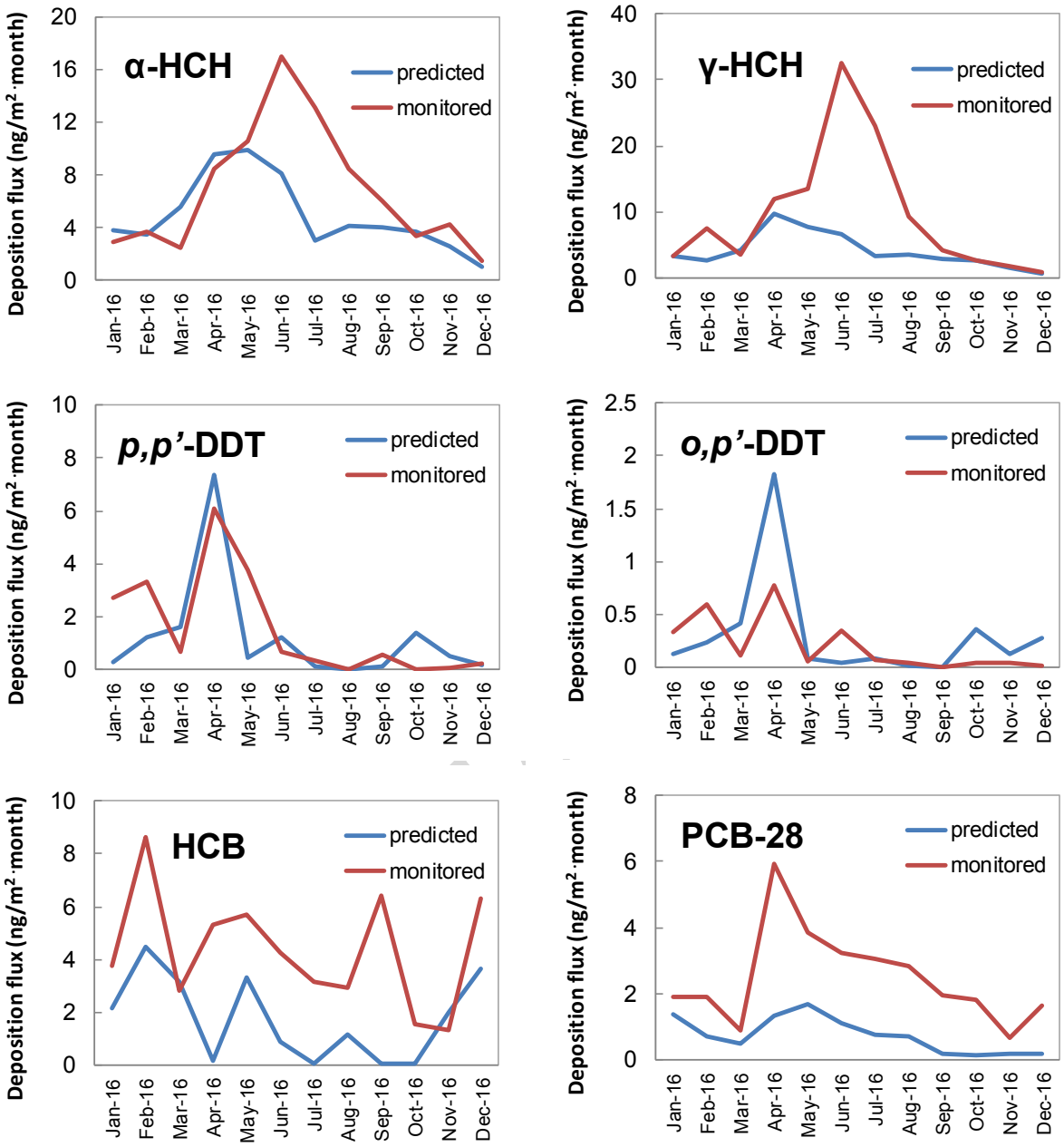

617

618 Fig. 4. Measured and predicted deposition fluxes at LNR

619